Erythropoietin Unfolding: Thermodynamics and Its Correlation with Structural Features[†]

Jurij Lah,[‡,*] Iztok Prislan,[‡] Blaž Kržan,[§] Mateja Salobir,[§] Andrej Francky,[§] and Gorazd Vesnaver[‡,*]

Faculty of Chemistry and Chemical Technology, University of Ljubljana, Askerceva 5, 1000 Ljubljana, Slovenia, and Lek Pharmaceuticals d. d., Verovskova 57, 1526 Ljubljana, Slovenia

Received July 6, 2005; Revised Manuscript Received August 19, 2005

ABSTRACT: Human erythropoietin (EPO) is a glycoprotein hormone considered to be the principal regulator of red blood cell formation. Although its recombinant version (rEPO) has been widely used for treatment of various anemias and its biological effects are relatively well-known, we know little about its biophysical properties and their relation to its structure. To gain a fuller understanding of the structural and functional properties of rEPO on the molecular level we followed its thermal and urea-induced unfolding at different pH (3.1−9.4) and urea concentrations (0−8 M) using spectropolarimetry, UV absorption, intrinsic emission fluorescence, and differential scanning calorimetry. Our results show that under a variety of conditions rEPO undergoes thermal or urea-induced denaturation that may be considered as a reversible two-state process characterized by unusually high (thermal) or moderate (urea-induced) extent of the residual structure. The highest thermal stability of the protein observed in aqueous solutions at physiological pH appears to be due to the largest difference in the extent of structure in the denatured and native state at this pH. The comparison between experimentally determined energetics of rEPO denaturation and its structure-based calculations indicates that the parametrization of thermodynamic quantities in terms of changes in solvent accessible nonpolar and polar surface areas resulting from protein unfolding can be successfully used provided that these changes are estimated from combination of experimentally determined ΔC°_{p} and ΔH° values and not calculated from the structure of the protein's folded and assumingly fully unfolded state.

Erythropoietin (EPO[1]), a glycoprotein hormone produced primarily in the kidney of adults, is the principal regulator of red blood cell production and differentiation (*1*, *2*). Since it is very difficult to obtain a sufficient amount of human urinary EPO for investigation of its chemical and biological properties, these studies are usually performed on recombinant erythropoietin (rEPO) that can be produced in a variety of host cells. The therapeutic importance of rEPO that is used worldwide for treating anemias derived from renal failure, chemotherapy, and AIDS has generated considerable interest in obtaining its structure−function characteristics (*3*). It has been shown that naturally occurring human EPO and also the rEPO secreted by the Chinese hamster ovary (CHO) cells contain three N-linked and one O-linked carbohydrates (*4*, *5*) which play an important role in the stability, solubility, and biological activity of the protein (*6*−*11*). The peptide moiety of both natural and recombinant EPO consists of 165 amino acids (*4*, *12*), and the average carbohydrate content in both proteins is about 40% (*13*, *14*). Such extensive glycosylation is probably the reason the structural information on EPO is rather scarce (*15*−*17*). The NMR-structural analysis performed recently on mutant rEPO (N24K, N38K, N83K) with lysine residues introduced at each of its N-linked glycosylation sites is to the best of our knowledge the only successful structural study on the uncomplexed rEPO (*15*). Since, in addition, practically no thermodynamic stability data on rEPO have been reported, one can conclude that general understanding of rEPO denaturation on the molecular level is rather poor. To obtain some better insight into the structural and functional properties of rEPO we decided to study its thermal and urea-induced denaturation by employing spectroscopic (CD, UV-absorption, fluorescence) and calorimetric (DSC) techniques. We attempted to correlate the measured Gibbs free energy, enthalpy, entropy, and heat capacity of denaturation with changes in the solvent accessible surface areas of rEPO that result from its complete unfolding and can be calculated from the available 3D structure of mutant rEPO (*15*). On the practical level our motivation for this work arises from the fact that the structural and thermodynamic information on the conformational changes of the protein is correlated to its functional properties. Since the formulations of drugs including rEPO as an active substance are patented at some specific conditions, our results may serve as preliminary information for designing a formulation of a generic drug at somewhat different conditions. To the best of our knowledge, this work represents the first attempt to characterize fully the thermodynamics of rEPO denaturation and to correlate it with the accompanying changes in the protein's structure.

[†] This work was supported by the Ministry of Science of Republic of Slovenia, Grant No. P1-0201, and by Lek Pharmaceuticals d. d. (Contract No. RR-1548/2003).

* Authors to whom correspondence should be addressed. G.V.: phone, +386 1 2419 402; fax, +386 1 2419 437; e-mail, gorazd.vesnaver@fkkt.uni-lj.si. J.L.: phone, +386 1 2419 414; fax, +386 1 2419 437; e-mail, jurij.lah@fkkt.uni-lj.si.

[‡] University of Ljubljana.

[§] Lek Pharmaceuticals d. d.

[1] Abbreviations: EPO, human erythropoietin; rEPO, recombinant version of human erythropoietin; DSC, differential scanning calorimetry; CD, circular dichroism; NMR, nuclear magnetic resonance.

10.1021/bi0512952 CCC: $30.25
Published on Web 09/28/2005

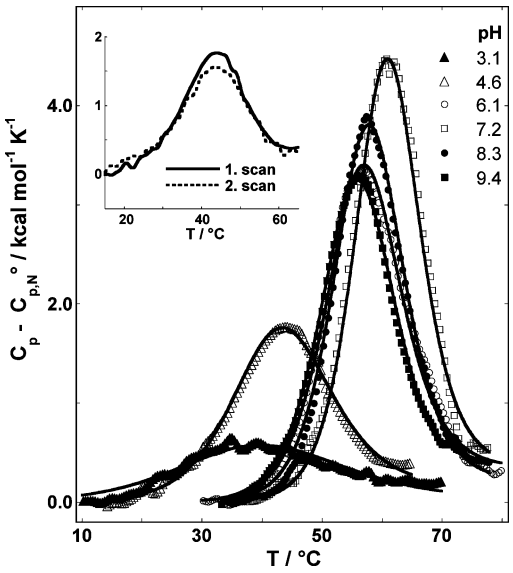

FIGURE 1: Thermal denaturation of rEPO monitored by DSC. In DSC thermograms measured at various pH the difference ($C_p - C_{p,N}$) between the raw signal corrected for the buffer contribution, C_p, and the heat capacity of the native state, $C_{p,N}$, is presented as a function of temperature. For clarity reasons only every fourth experimental point is presented. Full lines represent graphs of the best-fitted model function (eq 6). Inset: Reversibility test at pH = 4.6; full line, the first run; dotted line, the second run.

EXPERIMENTAL PROCEDURES

Materials. Recombinant erythropoietin, rEPO, was expressed from Chinese hamster ovary (CHO) cells and purified by ion exchange, reversed-phase, and gel filtration chromatography. Sample solutions of native rEPO were prepared by weighing the dry sample into the appropriate buffer solution. The extinction coefficient $\epsilon_{280} = 0.744$ mg^{-1} mL cm^{-1} determined at 25 °C in the phosphate buffer of pH = 7.2 is in good agreement with the corresponding literature value (*13*). In our work we were using the following buffer solutions which all contained 150 mM NaCl: 50 mM citrate (pH = 3.1), 50 mM acetate (pH = 4.6), 50 mM cacodylate (pH = 6.1), 50 mM phosphate (pH = 7.2), 50 mM TRIS (pH = 8.3), and 20 mM borate (pH = 9.4). All stock solutions of rEPO were dialyzed against the corresponding buffer solutions. For studying urea-induced denaturation of rEPO at a given temperature and pH, a number of rEPO solutions of constant protein and varying urea concentration (0−8 M) were prepared from the stock 10 M urea and rEPO solutions in the same buffer.

Differential Scanning Calorimetry (*DSC).* DSC was performed with a Nano-II DSC scanning calorimeter (CSC, UT). Thermal denaturation of rEPO (2.30 mg mL^{-1}) was monitored between pH = 3.1 and 9.4. A heating rate of 1 °C min^{-1} was used and it was shown that essentially the same results are obtained at a heating rate of 0.5 °C min^{-1}. The measured DSC thermograms presented at each pH as ($C_p - C_{p,N}$) versus T curves (Figure 1) were obtained by subtracting the heat capacity of the native state, $C_{p,N}$, from the raw signal corrected for the buffer contribution, C_p. The corresponding transition enthalpies, ΔH_{cal}, were calculated from the area under the ($C_p - C_{p,N}$) versus T curves. Due to the high ionization enthalpy of TRIS buffer (pH = 8.3, $\Delta H_{ion} = 11.3$ kcal mol^{-1}) the experiments at pH = 8.3 were repeated in HEPPS buffer ($\Delta H_{ion} = 5.0$ kcal mol^{-1}). The resulting thermodynamic parameters agreed within experimental error with those measured in TRIS, indicating that the contributions to ΔH_{cal} due to proton ionization may be neglected.

Circular Dichroism. CD spectra were recorded using a 62A DS AVIV spectropolarimeter (Aviv, Lakewood, NJ) equipped with a programmable, thermoelectrically controlled cell holder. Thermal denaturation of rEPO in the pH interval between 3.1 and 9.4 was monitored in the far-UV region through the measured ellipticity, Θ, versus T curves. Temperature dependence of the rEPO far-UV CD spectra corrected for solvent contributions was measured in several buffer solutions (pH interval 3.1−9.4) between 5 °C and 90 °C with a temperature step of 3 °C. Cuvettes of 0.1 cm path length were used, and the protein concentration was 0.34 mg mL^{-1}. Similarly, temperature dependence of the urea-induced (0−8 M) unfolding of rEPO at pH = 7.2 was followed at a number of temperatures between 10 °C and 40 °C by measuring the ellipticity at 225 nm.

UV Absorption. Absorbance spectra of rEPO in various buffer solutions were measured in a Cary 1 UV spectrophotometer equipped with a thermoelectrically controlled cell holder and a cell path of 1 cm. At each pH the temperature dependence of the rEPO absorbance spectra (0.55 mg mL^{-1}) was measured between 5 °C and 90 °C at intervals of 0.5 °C.

Spectrofluorimetry. Fluorescence (FL) emission spectra of rEPO were recorded between $\lambda_{em} = 300$ and 460 nm using a Perkin-Elmer LS 50 luminescence spectrometer (Perkin-Elmer, Buckingamshire, U.K.) equipped with a thermally controlled cell holder and a cuvette of 1 cm path length; λ_{ex} was 280 nm. Thermal denaturation of rEPO at a given pH (3.1−9.4) was followed by measuring the emission FL spectra between 10 °C and 85 °C with a temperature step of about 3 °C; the concentration of rEPO was around 0.04 mg mL^{-1}. Urea-induced denaturation of rEPO at pH = 7.2 was followed at several temperatures between 10 °C and 40 °C by measuring the rEPO fluorescence spectra at urea concentrations between 0 and 8 M (Figure 4a).

Model Analysis of Thermally and Urea-Induced Denaturation. The conformational stability of a globular protein that undergoes a reversible thermally or denaturant-induced denaturation that appears to be a two-state process,

$$\mathrm{N} \overset{K}{\leftrightarrow} \mathrm{D} \tag{1}$$

can be expressed in terms of the corresponding standard free energy change, ΔG°_T, as

$$\Delta G^\circ_T = -RT \ln K = -RT \ln \frac{\alpha}{1-\alpha} \tag{2}$$

where K is the equilibrium denaturation constant and α is the fraction of protein in the D state that depends on the temperature or denaturant concentration, respectively. Thermal denaturation is often characterized at some temperature T (usually 298 K), which is out of the temperature interval in which the true thermal unfolding occurs. The corresponding thermal stability expressed as ΔG°_T can be obtained by applying the Gibbs−Helmholtz equation,

$$\Delta G^\circ_T = T[\Delta H^\circ_{T_{1/2}}(1/T - 1/T_{1/2}) + \Delta C^\circ_p(1 - T_{1/2}/T - \ln(T/T_{1/2}))] \tag{3}$$

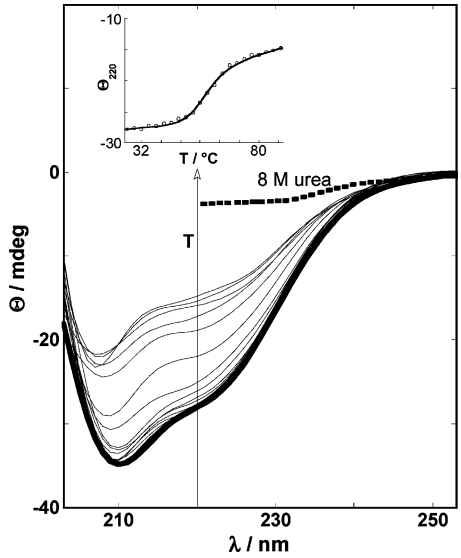

FIGURE 2: Thermal denaturation of rEPO monitored by spectropolarimetry (CD). Far-UV CD spectra of rEPO recorded between 5 °C and 90 °C at pH = 8.3. Bold line represents the CD spectrum measured at 25 °C after heating to 90 °C while the dotted line represents the CD spectrum observed at 25 °C and the same protein concentation in 8 M urea solution; protein concentration = 0.34 mg mL^{-1}. Inset: The corresponding melting curve constructed at 220 nm; full line represents the best-fitted model function (eq 5).

In this expression ΔG°_T refers to the N ↔ D transition projected from the temperature interval in which it actually occurs to the temperature T, $T_{1/2}$ is the melting temperature at which $\alpha = 0.5$, $\Delta H^\circ_{T_{1/2}}$ is the standard enthalpy of transition at $T_{1/2}$, and ΔC°_p is the difference in heat capacity between the unfolded and the folded state assumed to be independent of temperature. The corresponding ΔH°_T is determined from $\Delta H^\circ_T = \Delta H^\circ_{T_{1/2}} + \Delta C^\circ_p(T - T_{1/2})$ and then combined with ΔG°_T to obtain ΔS°_T.

Solvent-induced denaturation of globular proteins performed at a given temperature generally yields the corresponding ΔG°_T as a linear function of denaturant concentration,

$$\Delta G^\circ_T = \Delta G^\circ_{H_2O,T} - m[\text{denaturant}] \quad (4)$$

where $\Delta G^\circ_{H_2O,T}$ is an estimate of ΔG°_T in the absence of denaturant and m is an empirical parameter that correlates strongly with the amount of protein surface exposed to the solvent upon unfolding (*18*, *19*). As pointed out by Santoro and Bolen (*20*) $\Delta G^\circ_{H_2O,T}$ refers to the N ↔ D equilibrium that occurs at high denaturant concentrations projected to the limit of zero denaturant concentration, which means that $\Delta G^\circ_{H_2O,T}$ retains attributes of the N and D states existing at high denaturant concentrations. In other words, the quantities ΔG°_T (eq 3) and $\Delta G^\circ_{H_2O,T}$ (eq 4) that characterize thermal unfolding at low temperatures and denaturant-induced unfolding in the absence of denaturant refer to hypothetical unfolding reactions in which properties of both N and D are properties derived at high temperatures or high denaturant concentrations, respectively.

According to the reversible two-state model of protein denaturation (eqs 1, 2) one can express some physical property, F, that can be used for monitoring the denaturation process as

$$F = (1 - \alpha)F_N + \alpha F_D \quad (5)$$

where F_N and F_D are the F values characteristic of the pure N and D states, respectively. Depending on the method used for following the denaturation process, the quantity F used in this work was the measured ellipticity, the UV absorbance, the emission fluorescence intensity, and the standard partial molar enthalpy of the protein. In case of transitions followed by CD, absorbance, or fluorescence, the quantities F_N and F_D contained in the corresponding model function (eq 5) were assumed to be linear functions of temperature (thermal unfolding) or urea concentration (urea-induced unfolding). When thermal denaturation of proteins is followed by DSC, however, a partial derivation of eq 5 on T at constant pressure has to be applied to obtain an appropriate model function of the form (*21*−*26*)

$$C_p - C^\circ_{p,N} = \alpha\Delta C^\circ_p + \alpha(1 - \alpha)\{[\Delta H^\circ_{T_{1/2}} + \Delta C^\circ_p(T - T_{1/2})]^2/RT^2\} \quad (6)$$

in which $(C_p - C^\circ_{p,N})$ is the partial molar heat capacity of the protein relative to its native state. In an attempt to characterize thermodynamically the thermally induced denaturation of rEPO we followed eqs 1−3 and 5 or 6 and described the measured melting curves in terms of parameters $\Delta H^\circ_{T_{1/2}}$, $T_{1/2}$, and ΔC°_p. Their values were obtained from fitting the model function (eq 5 or 6) to the corresponding melting curves using the Levenberg−Marquardt nonlinear χ^2 regression procedure (*27*). Finally, these values of $\Delta H^\circ_{T_{1/2}}$, $T_{1/2}$, and ΔC°_p were used to calculate the ΔG°_T, ΔH°_T, and ΔS°_T of the protein's denaturation. By contrast, urea-induced denaturation of rEPO was followed at a number of temperatures by denaturation profiles (Figure 4) which were described by eqs 1, 2, 4, and 5 and used to obtain at each of the measured temperatures the corresponding $\Delta G^\circ_{H_2O,T}$ and m values. Equation 3 was fitted to these $\Delta G^\circ_{H_2O,T}$ values to obtain the parameters $\Delta H^\circ_{T_{1/2}}$, $T_{1/2}$, and ΔC°_p that characterize the hypothetical thermal unfolding of rEPO in the absence of urea that involves N and D states that would exist at high denaturant concentrations (*28*).

Numerous studies on protein stability performed in the past decade have shown that for protein unfolding both ΔH°_T and ΔC°_p can be parametrized in terms of the change in solvent accessible polar (ΔA_P) and nonpolar (ΔA_N) surface area associated with the unfolding process. Such parametrization is based on the calculation of the nonpolar (A_N) and polar (A_P) solvent accessible areas of proteins in the folded and the unfolded state that can be accomplished using the method introduced by Tsodikov et al. (*29*) A_N and A_P of native (folded) rEPO were obtained from the known NMR structure of mutant rEPO (*15*) using the probe size of 0.14 nm while the A_N and A_P values of the unfolded rEPO were estimated as the sum of the accessibilities of the protein residues located in the Ala-X-Ala tripeptides (*30*). ΔC°_p accompanying the unfolding of proteins can obtained from the parametrized equation (*31*)

$$\Delta C^\circ_p = 0.45[\text{cal mol}^{-1}\,\text{K}^{-1}\,\text{Å}^{-2}]\Delta A_N - 0.26[\text{cal mol}^{-1}\,\text{K}^{-1}\,\text{Å}^{-2}]\Delta A_P \quad (7)$$

while the corresponding enthalpy change, ΔH°_T, can be

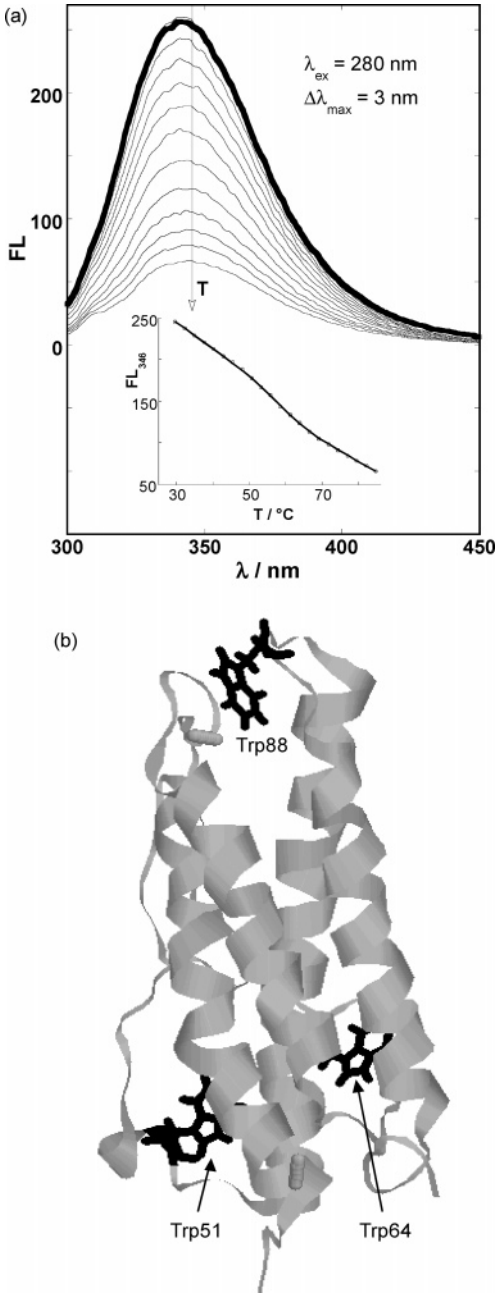

FIGURE 3: Thermal denaturation of rEPO monitored by intrinsic emmision fluorescence. (a) The temperature dependence of intrinsic fluorescence emission spectra measured between 10 °C and 86 °C at pH = 7.2 and the protein concentration of 0.033 mg mL^{-1}. Bold line represents the corresponding FL spectrum measured at 25 °C after heating to 85 °C, and $\Delta\lambda_{max}$ is the shift in λ_{max} observed upon heating the protein solution from 25 °C to 86 °C. Inset: The corresponding melting curve constructed at 346 nm; full line represents the best-fitted model function (eq 5). (b) The three-dimensional NMR solution structure of mutant rEPO in its native state (*15*). The Trp51 and Trp64 residues are seen to be buried within the core of the protein while the Trp88 residue appears to be partially exposed to the solvent.

estimated from the expression (*32*)

$$\Delta H^\circ_T = -8.44[\text{cal mol}^{-1}\ \text{Å}^{-2}]\Delta A_N + 31.4[\text{cal mol}^{-1}\ \text{Å}^{-2}]\Delta A_P + \Delta C^\circ_p(T - 333.15) \quad (8)$$

in which the sum of the two terms containing ΔA_N and ΔA_P represents the ΔH°_T value observed with most global proteins

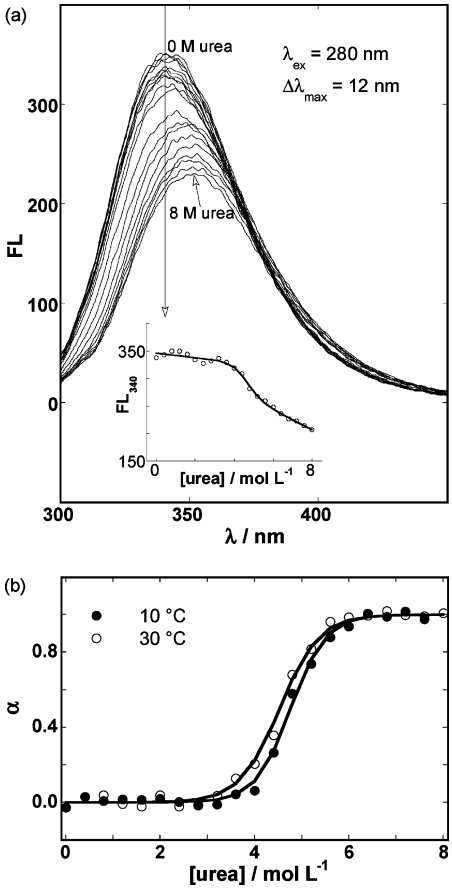

FIGURE 4: Denaturation of rEPO by urea. (a) The rEPO intrinsic fluorescence emission spectra measured at 30 °C, pH = 7.2, and protein concentration of 0.04 mg mL^{-1} at various urea concentrations between 0 and 8 M. $\Delta\lambda_{max}$ is the shift in λ_{max} observed upon changing the concentration of urea from 0 to 8 M. Inset: The corresponding urea-denaturation curve constructed at 340 nm; full line represents the best-fitted model function (eq 5). (b) The degree of urea-induced rEPO denaturation, α, determined at 10 °C and 30 °C from the corresponding CD urea-denaturation curves; full line represents the best-fitted model function (eq 5).

at their median transition temperature of 60 °C. The entropy change that accompanies the unfolding of proteins, ΔS°_T, can also be parametrized as (*33*):

$$\Delta S^\circ_T = \Delta S^\circ_{T,\text{solv}} + \Delta S^\circ_{\text{conf}} \quad (9)$$

The solvent contribution, $\Delta S^\circ_{T,\text{solv}}$, that describes the exposure of polar and nonpolar groups to the solvent upon unfolding of the protein can be expressed as $\Delta S^\circ_{T,\text{solv}} = \Delta C^\circ_p \ln(T/385.15)$ (*31*, *34*). The second term, $\Delta S^\circ_{\text{conf}}$, refers to the change in configurational entropy that results from the protein unfolding and can be estimated as $\Delta S^\circ_{\text{conf}} = \langle N\rangle 4.3$ cal K^{-1}(mol of residue)$^{-1}$ where $\langle N\rangle$ is the average number of amino acid residues participating in the unfolding process and 4.3 cal K^{-1} (mol of residue)$^{-1}$ is the average overall configuration entropy change obtained from the thermodynamic database for unfolding of monomeric proteins (*33*). Evidently, the number of amino acid residues involved in the unfolding process, $\langle N\rangle$, can be estimated from eq 9 using the corresponding experimentally determined ΔC°_p and ΔS°_T values.

As shown recently (*26*), the energetics of a protein denaturation can be correlated with its structural features through ΔA_N and ΔA_P values calculated from eqs 7 and 8

Table 1: Thermodynamic Parameters of rEPO Denaturation (N ↔ D) Obtained by Model Analysis of DSC Thermograms and Spectropolarimetric (CD) and UV Absorption (UV) Temperature Profiles

	$T_{1/2}$/°C			$\Delta H°_{T_{1/2}}$/kcal mol^{-1}				$\Delta C°_p$/kcal mol^{-1} K^{-1}
pH	DSC	CD	UV	cal[a]	DSC	CD	UV	DSC
3.1	40.4	38.0	40.9	19	21	20	20	0.02
4.6	43.0	43.4	39.7	36	37	35	28	0.15
6.1	56.5	56.5	55.9	52	53	48	45	0.35
7.2	60.6	60.8	60.8	62	62	60	62	0.35
8.3	57.6	57.5	55.8	55	57	53	54	0.22
9.4	55.9	55.6	54.7	50	52	51	57	0.15
error[b]	± 0.5	± 1	± 2	± 1	± 1	± 3	± 5	± 0.04

[a] Model-independent ΔH_{cal} values determined by integration of the corresponding DSC thermograms. [b] The errors were estimated from repetitive experiments by variation of possible baseline positions defining the initial (native) and the final (denatured) state. The errors obtained as square roots of diagonal elements of variance−covariance matrix by fitting of the corresponding model function (eq 5 or 6) to the individual melting curves are lower.

using the experimentally obtained values for $\Delta C°_p$ and $\Delta H°_T$. Furthermore, the average number of the unfolded residues, $\langle N \rangle$, can be estimated as

$$\langle N \rangle = (\Delta A_N + \Delta A_P)\langle N \rangle_{ST}/(\Delta A_{N,ST} + \Delta A_{P,ST}) \quad (10)$$

where the $(\Delta A_N + \Delta A_P)$ term refers to the ΔA_N and ΔA_P values calculated from eqs 7 and 8, the $(\Delta A_{N,ST} + \Delta A_{P,ST})$ term refers to those calculated for the complete unfolding from the structural data, and $\langle N \rangle_{ST}$ is the total number of residues contained in the protein.

RESULTS

The reversibility of thermal denaturation of rEPO in aqueous solutions was examined between pH = 3.1 and 9.4 by performing two consecutive DSC scans and by measuring CD and intrinsic fluorescence spectra after cooling the sample to the pretransitional temperature (Figures 1−3). Between pH = 4.6 and 8.3 the observed reversibility was better than 90% while at pH = 3.1 and 9.4 it dropped to about 70% and 80%, respectively (Table 1). The reversibility of urea-induced denaturation of rEPO was checked by diluting the rEPO solution in 8 M urea solution at pH = 7.2 with this particular buffer to pretransition urea concentrations and by comparing the CD and fluorescence spectra measured for these diluted solutions with those obtained for the same rEPO solutions prepared directly from urea and buffer of pH = 7.2. Again, the observed extent of reversibility was higher than 90%. According to the suggestions of Lopez and Makhatadze (*35*) the model-dependent parameters (eq 3) that describe the thermally induced denaturation of rEPO as a reversible two-state transition can be considered reliable only between pH = 4.6 and 8.3. At higher or lower pH their values can serve for comparative purposes.

Thermal Denaturation of rEPO

Differential Scanning Calorimetry (DSC). DSC thermograms measured between pH = 3.1 and 9.4 show single transitions characterized by the enthalpy of denaturation, ΔH_{cal}, and the transition temperature, $T_{1/2}$, that increase with increasing pH up to pH = 7.2 and then decrease with further increasing of pH to 9.4 (Figure 1). The measured model-independent ΔH_{cal} values agree well with the corresponding van't Hoff $\Delta H°_{T_{1/2}}$ values obtained from fitting the model function (eq 6) to the experimental $(C_p - C°_{p,N})$ vs T curves (Table 1).

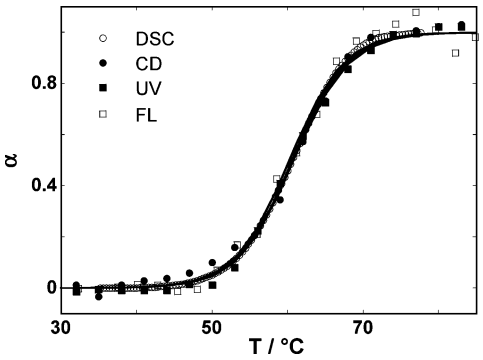

FIGURE 5: Thermal denaturation of rEPO followed by calorimetric and spectroscopic techniques. The degree of rEPO thermal denaturation, α, as a function of temperature determined at pH 7.2 from the DSC thermogram and the CD, UV, and FL melting curves; points represent the experimental values while the full lines represent the corresponding best fitted model function (eq 5).

Circular Dichroism (CD). Temperature dependence of the far-UV CD spectra measured between pH 3.1 and 9.4 shows a substantial decrease of the CD signal with increasing temperature (Figure 2). At room temperature a pronounced minimum in the CD spectrum at around 210 nm was observed at all measured pH. At the highest temperature of about 90 °C at which the thermal denaturation of rEPO appears to be completed this minimum is reduced only for about 30%. This observation strongly suggests that after undergoing a complete thermal denaturation rEPO retains a substantial amount of its secondary structure. As shown by the inset in Figure 2, the experimental Θ_λ vs T curves were constructed at each pH from the far-UV CD spectra measured at different temperatures. The corresponding model function (eq 5) based on the two-state model (eqs 1−3) was then fitted to these CD melting curves to obtain the characteristic parameters $\Delta H°_{T_{1/2}}$, $T_{1/2}$, and $\Delta C°_p$. The described fitting procedure resulted in reliable $\Delta H°_{T_{1/2}}$ and $T_{1/2}$ values that agree well with those obtained from the DSC experiments (Table 1). Unfortunately, the $\Delta C°_p$ adjustable parameter cannot be determined using this approach because fitting of the model function to the experimental optical melting curves turns out to be rather insensitive to $\Delta C°_p$.

Absorbance. Upon heating the rEPO solution from 5 °C to 90 °C its absorbance spectra show at all measured pH a drop in absorbance (λ_{max} = 282 nm) of only about 5%. Due to such low sensitivity of the measured absorbance to the temperature-induced conformational changes of rEPO, the corresponding UV melting curves cannot be considered as reliable as those constructed from the far-UV CD spectra. Nevertheless, fitting of the appropriate model function (eq 5) to these UV melting curves (not shown) results in adjustable parameters $\Delta H°_{T_{1/2}}$ and $T_{1/2}$ that are close to those obtained from DSC and CD experiments (Table 1, Figure 5).

Fluorescence. In contrast to the well-defined DSC and CD melting curves of rEPO, its emission fluorescence spectra show in all buffers almost linear decreasing of FL intensity with increasing temperature accompanied by a slight red shift

(≈3 nm) of the emission maximum (Figure 3). This result is consistent with the observed far-UV CD spectra of rEPO (Figure 2) which show that the thermally denatured rEPO contains a substantial amount of residual secondary structure and with the reported NMR structure of mutant rEPO (*15*) according to which the protein in its native state contains two Trp residues (Trp51, Trp64) that are buried within the core of the protein and one Trp residue (Trp88) that is partially (about 30%) exposed to the solvent (Figure 3b). If upon thermal denaturation rEPO retains most of its structure that contains the two buried Trp residues, the observed fluorescence intensity will change with temperature mainly due to its temperature quenching and to a smaller extent also due to a possible increase in exposure of the Trp88 residues that are partially exposed in the rEPO native state. One can expect that such thermal denaturation will be accompanied by only a minor red shift of the emission maximum. Inspection of Figure 3a shows full consistency between the suggested structural description of rEPO thermal denaturation and its experimental monitoring by fluorescence spectroscopy. It also shows that due to the shape of the melting curve its two state model analysis (eqs 1, 2, and 5) can only lead to qualitative thermodynamic data.

Denaturation of rEPO by Urea

Urea-induced denaturation of rEPO performed at pH = 7.2 was monitored by measuring the corresponding CD and intrinsic fluorescence spectra. CD monitoring in the far-UV region (Figure 2) indicates that the extent of the rEPO residual structure in the urea-denatured state is much lower than in its thermally denatured state. Similarly, fluorescence monitoring of urea-induced denaturation of rEPO at pH = 7.2 (Figure 4) results at high urea concentrations in a pronounced decrease of the emitted fluorescence and a red shift of the emission maximum (≈13 nm) that is substantially larger than the one observed with the thermal denaturation of rEPO in the same buffer solution in the absence of urea (≈3 nm, Figure 3). These observations indicate that upon urea denaturation the two Trp residues originally buried within the core of the protein become exposed to the aqueous environment to a much larger extent than upon thermal denaturation. In other words, the urea-induced denaturation of rEPO results in denatured states of the protein that contain considerably less residual structure than those obtained from the thermal denaturation. The urea-induced denaturation curves were constructed at each temperature from the measured far-UV CD and FL spectra (Figure 4) and then fitted with the model function (eq 5) combined with eqs 1, 2, and 4 to obtain the corresponding values of $\Delta G°_{H_2O,T}$ and m. The model function (eq 3) was then fitted to these $\Delta G°_{H_2O,T}$ to estimate parameters $\Delta H°_{T_{1/2}}$, $T_{1/2}$, and $\Delta C°_p$ that characterize the hypothetical thermal denaturation of rEPO, which involves its native and denatured states projected from high urea concentrations (Figure 7).

DISCUSSION

The denaturation of rEPO under the conditions used in this study was assumed to be a reversible two-state process. There are several possibilities to check the validity of this assumption (*36*−*39*). In the case of thermal denaturation the most rigorous way of confirming it is to use DSC and compare the corresponding directly measured enthalpies of transition to the van't Hoff enthalpies calculated from the

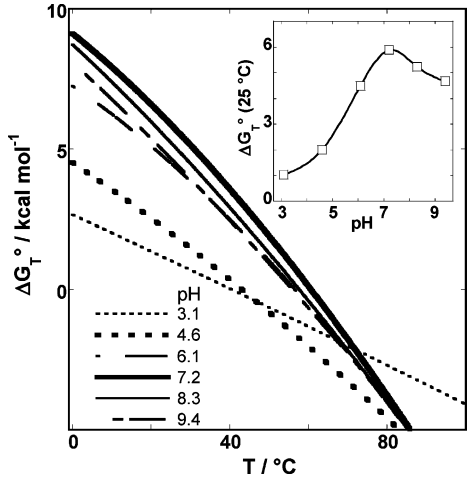

FIGURE 6: Thermodynamic stability of rEPO as a function of pH. $\Delta G°_T$ of rEPO thermal denaturation as a function of temperature (eq 3) determined at various pH from the corresponding DSC thermograms. Inset: The pH profile of $\Delta G°_T$ at 25 °C.

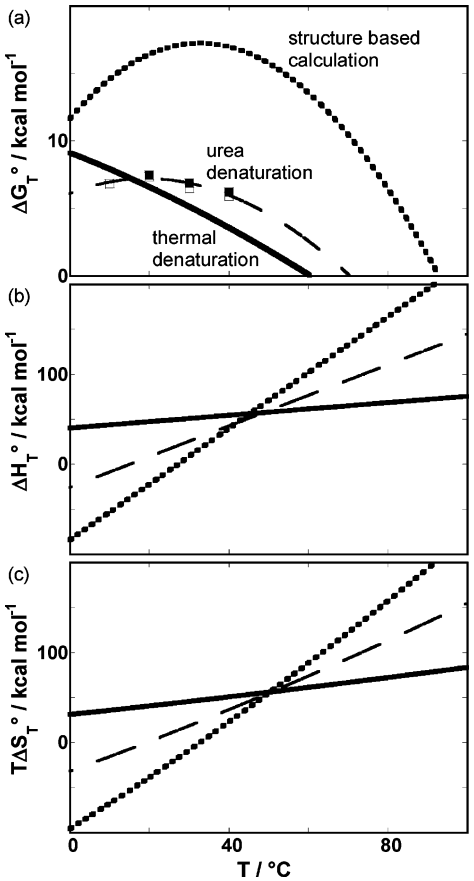

FIGURE 7: Thermodynamic stability of rEPO at pH = 7.2. $\Delta G°_T$, $\Delta H°_T$, and $T\Delta S°_T$ of rEPO denaturation as a function of temperature obtained from thermally induced (DSC, pH = 7.2; full line) and urea-induced denaturation (pH = 7.2, disconnected line) in comparison with the corresponding quantities estimated from the structure-based calculations (dotted line; eqs 7−9 for $\Delta A_{N,ST}$ = 10 362 Å^2, $\Delta A_{P,ST}$ = 6027 Å^2, and $\langle N \rangle_{ST}$ = 165). (a) $\Delta G°_T$ as a function of T. Values of $\Delta G°_T$ extrapolated to zero urea concentration ($\Delta G°_{H_2O,T}$) were obtained from urea denaturation curves monitored by CD (□) and fluorescence (■) spectroscopy. The disconnected line is the best fit of eq 3 to these $\Delta G°_T$ ($T_{1/2}$ = 94 °C, $\Delta H°_{T_{1/2}}$ = 70 kcal mol^{-1}, $\Delta C°_p$ = 1.7 kcal mol^{-1}). (b) $\Delta H°_T$ as a function of T. (c) $T\Delta S°_T$ as a function of T.

DSC thermograms and spectroscopic melting curves using the two-state approximation. Good agreement between the model-independent and model-dependent enthalpies of transition observed with rEPO thermal denaturation (Table 1) clearly shows that thermal denaturation of rEPO may be considered as a two-state transition. This observation is further confirmed by the fact that all experimental techniques used for monitoring the thermal denaturation of rEPO resulted in the same two-state transition curve (Figure 5). For denaturant-induced denaturation, however, there is no rigorous way of confirming the assumed two-state mechanism. In this study we monitored denaturation by several spectroscopic methods and checked the coincidence of the results derived from the observed denaturation curves assuming the two-state transition mechanism. We followed the urea-induced denaturation of rEPO by far-UV CD and intrinsic fluorescence spectroscopy (Figure 4). Good agreement between the experimental denaturation curves and the corresponding model function (eqs 1, 2, and 5) observed with both experimental techniques indicates that urea-induced denaturation of rEPO may also be considered as a two-state transition. Finally, the validity of the two-state assumption for the thermal and urea-induced denaturation monitored by spectroscopic methods was checked by the dual wavelength parametric test (*39*). The obtained linear parametric CD, UV absorption, and fluorescence plots indicate that the observed conformational transitions can be considered as two-state processes.

Analysis of thermal denaturation experiments (Figures 1−3) indicates that the stability of rEPO strongly depends on pH. In the studied temperature interval the measured free energy of denaturation ΔG°_T exhibits a maximum at pH around 7.2 (Figure 6) and agrees well with the corresponding values reported by Arakawa et al. (*40*). At all measured pH the corresponding ΔH°_T and ΔS°_T show that enthalpic and entropic contributions to ΔG°_T are about equally important. Table 1 shows that ΔC°_p depends strongly on pH. Since ΔC°_p measures primarily the increase in hydration upon unfolding, the observed changes in ΔC°_p that accompany changes in pH argue for corresponding major structural changes in either the native state, the denatured state, or both. The relative reduction of rEPO structure that results from thermal denaturation in the measured pH interval expressed at each pH as the difference between the Θ_{220} values measured at 86 °C and 5 °C, respectively, is presented in Figure 8a. The feature of these data argues rather strongly that at low and high pH the extent of the reduced secondary structure upon denaturation is significantly lower than at neutral pH. It seems that at low or high pH the native state of rEPO with the surplus of positive or negative charge is due to the increased repulsion of the like charges less structured than at physiological pH. The same should be true also for the denatured rEPO since an unfolded protein with a surplus of positive or negative charge would also tend to be more extended than the neutral protein. As shown in Figure 8a, the described electrostatic repulsion effect is more pronounced with the native state of rEPO (smaller difference between Θ_{220} values of unfolded and folded state), and because of that the thermal denaturation of rEPO performed at low or high pH results in reduced ΔC°_p values.

Temperature dependence of rEPO stability at pH = 7.2 (ΔG°_T vs T curves) obtained from thermal and urea-induced denaturation together with the corresponding enthalpy and entropy contributions is presented in Figure 7. The ΔG°_T values obtained from urea-induced denaturation ($\Delta G^\circ_T = \Delta G^\circ_{H_2O,T}$, see Experimental Procedures) around the physiological temperature appear to be more positive than those obtained from thermal denaturation. These differences are rather small due to the effective compensation of ΔH°_T and $T\Delta S^\circ_T$ contributions, which are for urea-induced denaturation of rEPO much larger than for its thermal denaturation (Figure 7). Since in the urea-denatured state the extent of the secondary structure appears to be significantly lower than in the thermally denatured state (Figures 2−4), the observed differences in ΔG°_T, ΔH°_T, and $T\Delta S^\circ_T$ may be attributed in the first place to the enhanced hydrophobic contribution to these quantities. As suggested by many authors, this enhancement results from the increased number of unfolded residues in the urea-denatured state accompanied by an increase in the solvent accessible area of the protein and a consequent increase in its hydration (*19*, *26*, *31*, *32*, *41*−*43*). Such explanation is clearly supported by the fact that ΔC°_p obtained from the urea denaturation (1.7 kcal mol^{-1} K^{-1}) substantially exceeds its value determined from the thermal denaturation (0.35 kcal mol^{-1} K^{-1}).

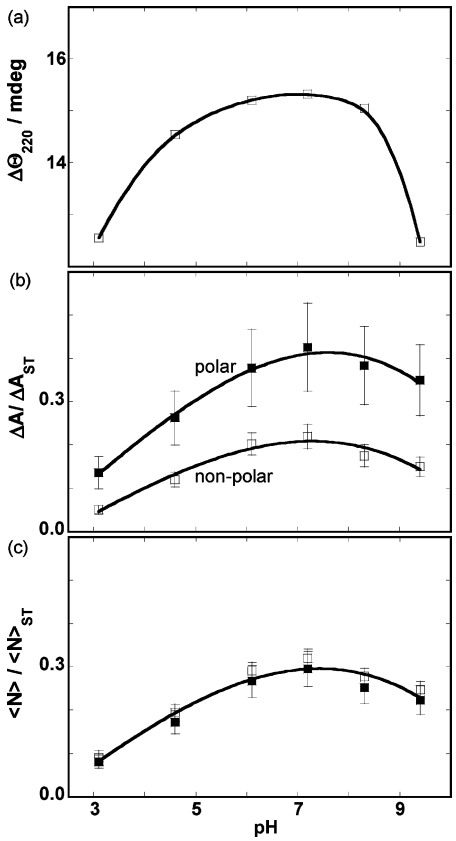

FIGURE 8: pH dependence of rEPO structural characteristics. (a) Change in the measured ellipticity, $\Delta\Theta_{220}$, upon heating the rEPO solution from 5 °C to 86 °C (rEPO concentration = 0.34 mg mL^{-1}). (b) The changes in nonpolar, ΔA_N, and polar, ΔA_P, solvent accessible surfaces upon rEPO denaturation estimated from experimentally obtained data (Table 1) and eqs 7 and 8 are given relative to $\Delta A_{N,ST}$ and $\Delta A_{P,ST}$ obtained for "complete unfolding" (transition to Ala-X-Ala denatured state, $\Delta A_{N,ST}$ = 10 362 Å^2, $\Delta A_{P,ST}$ = 6027 Å^2). (c) The number of amino acid residues participating in the unfolding, $\langle N \rangle$, estimated from eqs 9 (□) and 10 (■) relative to the total number of structured residues, $\langle N \rangle_{ST}$ = 165, in rEPO.

In an attempt to correlate protein structural features to the thermodynamics of its unfolding, several authors have proposed an empirical parametrization approach in which structure-based calculations of thermodynamic quantities of denaturation are based largely upon the accompanying increase in exposure of the protein's nonpolar, A_N, and polar, A_P, surface areas to the solvent (*19*, *31*, *32*, *41*−*43*). In this study we used the parametrization (*31*, *32*) according to which the characteristic quantities of unfolding ΔC°_p and ΔH°_T are expressed only in terms of the corresponding ΔA_N and ΔA_P (eqs 7 and 8). Following the already described structure-based procedure of estimating the A_N and A_P of rEPO in its native and completely unfolded state, we first determined these values, and then by subtracting them we obtained the corresponding changes $\Delta A_{N,ST} = 10\,362$ Å^2 and $\Delta A_{P,ST} = 6027$ Å^2, which were further used to calculate from eqs 7 and 8 the corresponding structure-based values of $\Delta C^\circ_{p,ST}$ and $\Delta H^\circ_{T,ST}$. By employing eq 9 in which $\Delta S^\circ_{T,solv} = \Delta C^\circ_{p,ST} \ln(T/385.15)$ and $\Delta S^\circ_{conf} = \langle N\rangle_{ST} 4.3$ cal K^{-1} (mol of residue)$^{-1}$, we obtained the stucture-based value of $\Delta S^\circ_{T,ST}$, which combined with $\Delta H^\circ_{T,ST}$ resulted in the corresponding $\Delta G^\circ_{T,ST}$ (*31*−*34*). As can be seen from Figure 7, the free energy, enthalpy, and entropy of rEPO unfolding obtained from these structure-based calculations do not agree well with those obtained from the experiment (eqs 1−3, 6). Moreover, the calculated $\Delta C^\circ_{p,ST} = 3.1$ kcal mol^{-1} K^{-1} is much higher than the highest experimental ΔC°_p of 0.35 kcal mol^{-1} K^{-1} determined at pH = 7.2. At lower or higher pH the agreement between the calculated and experimental ΔC°_p values is even worse. In our opinion the observed discrepancies are not surprising because the estimation of the structural parameters $\Delta A_{N,ST}$ and $\Delta A_{P,ST}$ is always questionable due to the problem of defining the structure of the initial and final state of the protein. For initial states the NMR and X-ray structures are often known, and thus their A_N and A_P can be calculated using well-known methods (*29*, *44*−*46*). The problem with the initial state is that we usually know its structure only at given conditions (*T*, pH, ionic strength, solid state, and so on). So, when we study protein unfolding at some other conditions, for example at much lower or higher pH, the structure of its initial state and the corresponding A_N and A_P may be significantly different from those at neutral pH. There is another, even more difficult problem with the final state of the protein which is assumed to be in a random coil conformation and thus characterized by an unfolded polypeptide chain that has to be approximated by a certain model (see for example ref *41* and the corresponding references therein). In numerous studies dealing with the determination of the solvent accessible surface area of the unfolded state, A_N and A_P are estimated by calculating the surface area of each amino acid residue located in an extended tripeptide, Ala-X-Ala (as in this study) or Gly-X-Gly, and then summing these contributions over all the residues contained by the protein. Such estimation implies a completely extended unfolded protein. If the denatured protein does not exist in such a state, the described procedure may result in an overestimation of its solvent accessible surface areas A_N and A_P. As a consequence, the protein's $\Delta A_{N,ST}$ and $\Delta A_{P,ST}$ are overestimated and the result is an overestimation of $\Delta C^\circ_{p,ST}$.

As shown recently, the correlation of the experimentally determined thermodynamics of thermal or urea-induced denaturation of rEPO with its structural features can be carried out using an opposite approach (*26*) in which ΔA_N, ΔA_P, and $\langle N\rangle$ that accompany denaturation of rEPO are calculated from combination of experimental thermodynamic data and parametrized eqs 7−9. These calculations show that upon thermal denaturation of rEPO in the measured pH interval the ratios $\Delta A_N/\Delta A_{N,ST}$ and $\Delta A_P/\Delta A_{P,ST}$ increase from about 15% and 5% at pH = 3.1 to about 40% and 20% at pH = 7.2 and then drop to about 35% and 15% at pH = 9.4 (Figure 8b). Similarly, the $\langle N\rangle/\langle N\rangle_{ST}$ ratio in which $\langle N\rangle$ is determined either from eq 9 or 10 increases from about 10% at pH = 3.1 to about 30% at pH = 7.2 and drops again to about 20% at pH = 9.4 (Figure 8c). For the hypothetical thermal denaturation of rEPO followed at pH = 7.2 in which the native and denatured states are those projected from high urea concentrations, the described calculations result in $\Delta A_N/\Delta A_{N,ST} = 59\%$, $\Delta A_P/\Delta A_{P,ST} = 68\%$, and $\langle N\rangle/\langle N\rangle_{ST} = 65\%$ (eq 9) or 63% (eq 10). Evidently, these $\Delta A_N/\Delta A_{N,ST}$, $\Delta A_P/\Delta A_{P,ST}$, and $\langle N\rangle/\langle N\rangle_{ST}$ values show that the degree of thermally induced unfolding of rEPO is unexpectedly low. They also show that thermally denatured state of rEPO is significantly less unfolded than its urea-denatured state which is in line with our far-UV CD and fluorescence results (Figures 2−4) and with the generally accepted observation that urea-denatured proteins have less residual structure than thermally denatured proteins (*47*). Finally, they are fully consistent with our suggestion made earlier that the observed large discrepancy between the experimentally determined ΔG°_T, ΔH°_T, and ΔS°_T of rEPO denaturation and the corresponding $\Delta G^\circ_{T,ST}$, $\Delta H^\circ_{T,ST}$, and $\Delta S^\circ_{T,ST}$ obtained from the structure-based calculations is mainly due to the incomplete unfolding of rEPO upon denaturation and at low or high pH also to a partially unfolded native state. We are well aware that the ΔA_N, ΔA_P, and $\langle N\rangle$ values determined from the described combination of experimental thermodynamics and structure-based parametrization can be considered only as reasonably good approximations since they comprise errors of the empirical parametrization and those of the measured thermodynamic quantities. Nevertheless, we believe that using this approach one can explain, at least in a semiquantitative way, the observed thermally induced or urea-induced denaturation of rEPO. We would like to point out that the excellent agreement between the $\langle N\rangle$ values obtained from independent parametrization of ΔC°_p and ΔH°_T (eqs 7, 8) combined with eq 10 on one side and from the parametrization of ΔS°_T (eq 9) on the other (Figure 8c) strongly supports the suggested parametrization of the quantities ΔC°_p, ΔH°_T, and ΔS°_T (eqs 7−9) provided they are parametrized in terms of the "true" ΔA_N and ΔA_P values. Considering the above, we believe that for proteins with poorly defined structure of native and/or denatured state attempts to correlate the experimental thermodynamics of protein denaturation with its structural features would benefit from this kind of approach.

ACKNOWLEDGMENT

We are especially grateful to the Biopharmaceutics Lek team for developing the protocol for rEPO expression and purification. They prepared the protein in the amounts needed for this biophysical study.

REFERENCES

1. Graber, S. E., and Krantz, S. B. (1978) Erythropoietin and control of red-cell production, *Annu. Rev. Med. 29*, 51−66.

2. Krantz, S. B., and Goldwasser, E. (1984) Specific binding of erythropoietin to spleen-cells infected with the anemia strain of friend-virus, *Proc. Natl. Acad. Sci. U.S.A. 81*, 7574−7578.
3. Markham, A., and Bryson, H. M. (1995) Epoetin alfa—a review of its pharmacodynamic and pharmacokinetic properties and therapeutic use in nonrenal applications, *Drugs 49*, 232−254.
4. Lai, P.-H., Everett, R., Wang, F.-F., Arakawa, T., and Goldwasser, E. (1986) Structural characterization of human erythropoietin, *J. Biol. Chem. 261*, 3116−3121.
5. Takeuchi, M., Takasaki, S., Miyazaki, H., Kato, T., Hoshi, S., Kochibe, N., and Kobata, A. (1988), Comparative study of the asparagine-linked sugar chains of human erythropoietins purified from urine and the culture medium of recombinant chinese hamster ovary cells, *J. Biol. Chem. 263*, 3657−3663.
6. Dordal, M. S., Wang, F. F., and Goldwasser, E. (1985) The role of carbohydrate in erythropoietin action, *Endocrinology 116*, 2293−2299.
7. Goldwasser, E., Kung, C. K.-H., and Eliason, J. (1974) Mechanism of erythropoietin-induced differentiation. 13. Role of sialic-acid in erythropoietin action, *J. Biol. Chem. 249*, 4202−4206.
8. Takeuchi, M., Inoue, N., Strickland, T. W., Kubota, M., Wada, M., Shimizu, R., Hoshi, S., Kozutsumi, H., Takasaki, S., and Kobata, A. (1989) Relationship between sugar chain structure and biological-activity of recombinant human erythropoietin produced in chinese-hamster ovary cells, *Proc. Natl. Acad. Sci. U.S.A. 86*, 7819−7822.
9. Takeuchi, M., Takasaki, S., Shimada, M., and Kobata, A. (1990) Role of sugar chains in the invitro biological-activity of human erythropoietin produced in recombinant chinese hamster ovary cells, *J. Biol. Chem. 265*, 12127−12130.
10. Tsuda, E., Kowanishi, G., Ueda, M., Masuda, S., and Sasaki, R. (1990) The role of carbohydrate in recombinant human erythropoietin, *Eur. J. Biochem. 188*, 405−411.
11. Goto, M., Akai, K., Murakami, A., Hashimoto, C., Tsuda, E., Ueda, M., Kawanishi, G., Takahashi, N., Ishimoto, A., Chiba, H., and Sasaki, R. (1988) Production of recombinant human erythropoietin in mammalian-cells—host-cell dependency of the biological-activity of the cloned glycoprotein, *Bio/Technology 6*, 67−71.
12. McDonald, J. D., Lin, F.-K., and Goldwasser, G. (1986) Cloning, sequencing, and evolutionary analysis of the mouse erythropoietin gene, *Mol. Cell. Biol. 6*, 842−848.
13. Davis, J. M., Arakawa, T., Strickland, T. W., and Yphantis, D. H. (1987) Characterization of recombinant human erythropoietin produced in chinese hamster ovary cells, *Biochemistry 26*, 2633−2638.
14. Kolvenbach, C. G., Langley, K. E., Strickland, T. W., Kenney, W. C., and Arakawa, T. (1991) Densitometric determination of carbohydrate content in glycoproteins, *J. Biochem. Biophys. Methods 23*, 295−300.
15. Cheetham, J. C., Smith, D. M., Aoki, K. H., Stevenson, J. L., Hoeffel, T. J., Syed, R. S., Egrie, J., and Harvey, T. S. (1998) NMR structure of human erythropoietin and a comparison with its receptor bound conformation, *Nat. Struct. Biol. 5*, 861−866.
16. Syed, R. S., Reid, S. W., Li, C., Cheetham, J. C., Aoki, K. H., Liu, B., Zhan, H., Osslund, T. D., Chirino, A. J., Zhang, J., Finer-Moore, J., Elliot, S., Sitney, K., Katz, B. A., Matthews, D. J., Wendoloski, J. J., Egrie, J., and Stroud, R. M. (1998) Efficiency of signalling through cytokine receptors depends critically on receptor orientation, *Nature 395*, 511−516.
17. Livnah, O., Johnson, D. L., Stura, E. A., Farrell, F. X., Barbone, F. P., You, Y., Liu, K. D., Goldsmith, M. A., He, W., Krause, C. D., Pestka, S., Jolliffe, L. K., and Wilson, I. A. (1998) An antagonist peptide-EPO receptor complex suggests that receptor dimerization is not sufficient for activation, *Nat. Struct. Biol. 5*, 993−1004.
18. Schellman, J. A. (1978) Solvent denaturation, *Biopolymers 17*, 1305−1322.
19. Myers, J. K., Pace, N. C., and Scholtz, M. J. (1995) Denaturant m-values and heat-capacity changes—relation to changes in accessible surface areas of protein unfolding, *Protein Sci. 4*, 2138−2148.
20. Santoro, M. M., and Bolen, D. W. (1992). A test of a linear extrapolation of unfolding free energy changes over an extended denaturant concentration range, *Biochemistry 31*, 4901−4907.
21. Freire, E., and Biltonen, R. L. (1978) Statistical mechanical deconvolution of thermal transitions in macromolecules. 1. Theory and application to homogeneous systems, *Biopolymers 17*, 463−479.
22. Privalov, P. L., and Pothekin, S. A. (1986) Scanning Microcalorimetry in Studying Temperature-induced Changes in Proteins, *Methods Enzymol. 131*, 4−51.
23. Freire, E. (1989) Statistical Thermodynamic Analysis of the Heat Capacity Function Associated with Protein Folding-Unfolding Transitions, *Comments Mol. Cell. Biophys. 6*, 123−140.
24. Lah, J., Marianovsky, I., Glaser, G., Engelberg-Kulka, H., Kinne, J., Wyns, L., and Loris, R. (2003) Recognition of the intrinsically flexible addiction antidote MazE by a dromedary single-domain antibody fragment: Structure, thermodynamics of binding, stability and influence on interactions with DNA, *J. Biol. Chem. 278*, 14101−14111.
25. Lah N., Lah, J., Zegers, I., Wyns, L., and Messens, J. (2003) Specific potassium binding stabilizes pI258 arsenate reductase from *S. aureus*, *J. Biol. Chem. 278*, 24673−24679.
26. Lah, J., Simic, M., Vesnaver, G., Marianovsky, I., Glaser, G., Engelberg-Kulka H., and Loris, R. (2005) Energetics of structural transitions of the addiction antitoxin MazE—Is a programmed bacterial cell death dependent on the intrinsically flexible nature of the antitoxins?, *J. Biol. Chem. 280*, 17397−17407.
27. Press, W. H., Flannery, B. P., Teukolsky, S. A., and Vetterling, W. T. (1992) *Numerical Recipies*, Cambridge University Press, Oxford, pp 650−694.
28. Dao-Thi, M.-H., Messens, J., Wyns, L., and Backmann, J. (2000) The thermodynamic stability of the proteins of the *ccd* plasmid addiction system, *J. Mol. Biol. 299*, 1373−1386.
29. Tsodikov, O. V., Record, M. T., and Sergeev, Y. V. (2002) Novel computer program for fast exact calculation of accessible and molecular surface areas and average surface curvature, *J. Comput. Chem. 23*, 600−609.
30. Murphy, K. P., Bhakuni, V., Xie, D., and Freire, E. (1992) Molecular basis of co-operativity in protein folding. 3. Structural identification of cooperative folding units and folding intermediates, *J. Mol. Biol. 227*, 293−306.
31. Murphy. K. P., and Freire, E. (1992) Thermodynamics of structural stability and cooperative folding behavior in proteins, *Adv. Protein Chem. 43*, 313−361.
32. Xie, D., and Freire, E. (1994) Molecular basis of cooperativity in protein folding. 5. Thermodynamic and structural conditions for the stabilization of compact denatured states, *Proteins: Struct., Funct., Genet. 19*, 291−301.
33. Lee, K. H., Xie, D., Freire, E., and Amzel, M. (1994) Estimation of changes in side chain configurational entropy in binding and folding: General methods and applications to helix formation, *Proteins: Struct., Funct., Genet. 20*, 68−84.
34. Baldwin, R. L. (1986) Temperature dependence of the hydrophobic interaction in protein folding, *Proc. Natl. Acad. Sci. U.S.A. 83*, 8069−8072.
35. Lopez, M. M., and Makhatadze, G. I. (2002) Differential scanning calorimetry, *Methods Mol. Biol. 173*, 113−119.
36. Lumry, R., Biltonen, R., and Brandts, J. F. (1966) Validity of the "two-state" hypothesis for conformational transitions of proteins, *Biopolymers 4*, 917−944.
37. Chaires, J. B. (1997) Possible origin of differences between van't Hoff and calorimetric enthalpy estimates, *Biophys. Chem. 64*, 15−23.
38. Horn, J. R., Russel, D., Lewis, E. A., and Murphy, K. P. (2001) van't Hoff and calorimetric enthalpies from isothermal titration calorimetry: Are there significant discrepancies?, *Biochemistry 40*, 1774−1778.
39. Wallimann, P., Kennedy, R. J., Miller, J. S., Shalongo, W., and Kemp, D. S. (2003) Dual wavelength parametric test of two state models for circular dichroism spectra of helical polypeptides: Anomalous dichroic properties of alanine-rich peptides, *J. Am. Chem. Soc. 125*, 1203−1220.
40. Arakawa, T., Philo, J. S., and Kita, Y. (2001) Kinetic and thermodynamic analysis of thermal unfolding of recombinant erythropoietin, *Biosci., Biotechnol., Biochem. 65*, 1321−1327.
41. Makhatadze, G. I., and Privalov, P L. (1995) Energetics of protein structure, *Adv. Protein Chem. 47*, 307−425.
42. Loladze, V. V., Ermolenko, D. N., and Makhatadze, G. I. (2001) Heat capacity changes upon burial of polar and nonpolar groups in proteins, *Protein Sci. 10*, 1343−1352.
43. Spolar, R. S., and Record, M. T., Jr. (1994) Coupling of local folding to site-specific binding of proteins to DNA, *Science 263*, 777−784.

44. Lee, B., and Richards, F. M. (1971) The interpretation of protein structures: Estimation of static accessibility, *J. Mol. Biol. 55*, 379−400.
45. Hubbard, S. J., and Thornton, J. M. (1993) *NACCESS computer program*, University College London.
46. Liang, H., Sandberg, W. S., and Terwillinger, T. C. (1993) Genetic fusion of subunits of a dimeric protein substantially enhances its stability and rate of folding, *Proc. Natl. Acad. Sci. U.S.A. 90*, 7010−7014.
47. Tanford, C. (1968) Protein denaturation, *Adv. Protein Chem. 23*, 121−282.

BI0512952